State-of-Charge Estimation of NMC-based Li-ion Battery Based on Continuous Transfer Function Model and Extended Kalman Filter

Naseri, Farshid; Schaltz, Erik; Stroe, Daniel Ion; Gismero, Alejandro; Farjah, Ebrahim; Karimi, Sepehr

Published in:
2021 12th Power Electronics, Drive Systems, and Technologies Conference, PEDSTC 2021

DOI (link to publication from Publisher):
10.1109/PEDSTC52094.2021.9405847

Publication date:
2021

Document Version
Accepted author manuscript, peer reviewed version

State-of-Charge Estimation of NMC-based Li-ion Battery Based on Continuous Transfer Function Model and Extended Kalman Filter

Farshid Naseri
Dep. of Power & Control Engineering
School of ECE, Shiraz University
Shiraz, Iran
f.naseri@shirazu.ac.ir

Erik Schaltz
Department of Energy Technology
Aalborg University
Aalborg, Denmark
esc@et.aau.dk

Daniel-Ion Stroe
Department of Energy Technology
Aalborg University
Aalborg, Denmark
dis@et.aau.dk

Alejandro Gismero
Department of Energy Technology
Aalborg University
Aalborg, Denmark
aga@et.aau.dk

Ebrahim Farjah
Dep. of Power & Control Engineering
School of ECE, Shiraz University
Shiraz, Iran
farjah@shirazu.ac.ir

Sepehr Karimi
Dep. of Power & Control Engineering
School of ECE, Shiraz University
Shiraz, Iran
sepehrkarimi72@gmail.com

***Abstract*— Lithium-ion (Li) battery based on nickel-manganese-cobalt (NMC) cathode has emerged as one of the most successful battery types for powertrain of Electric Vehicles (EVs). The effective management of the NMC-based battery relies on accurate estimation of its State-of-Charge (SoC) in the Battery Management System (BMS). In this paper, an effective system identification approach is applied to establish the battery model using a Continuous Transfer Function (CTF) model. The Akaike information criterion (AIC) is applied to obtain the suitable model structure considering the accuracy and real-time efficiency of the model. Then, the SoC Estimation is fulfilled based on the developed model and the Extended Kalman Filter (EKF) algorithm. The correct performance of the proposed method is evaluated and confirmed using experimental data of 3.4 Ah 3.7 V NMC-based battery cells. Likewise, the feasibility of embedded implementation is proven through some Hardware-in-the-Loop (HiL) tests.**

Keywords*— *Battery Management System (BMS), System Identification, State Estimation

I. INTRODUCTION

Recent advancements in Lithium-ion (Li-ion) battery technology has fueled the electrification of the transportation sector and in particular the Electric Vehicles (EVs) development [1]. Despite the great investments and achievements that have been fulfilled in this sector, high cost of the EV battery pack and its limited life span still remain to be the biggest challenges for deployment of electrical Mobility in the world [2]. In this context, the Li-ion battery based on nickel-manganese-cobalt (NMC) cathode has shown to provide promising performance characteristics in vehicular applications [3]. Apart from the battery technology, another critical element is the Battery Management System (BMS), which is responsible for monitoring, controlling, and protecting the EV battery pack. The core component of the BMS is the State-of-Charge (SoC) estimation mechanism, which reflects the remaining energy (in terms of Ampere-hour) of the battery. In the BMS, the information of SoC is usually used to fulfill objectives like cell-balancing, protection of the cells, EV range estimation, etc. Thus, the SoC estimation error should be low enough to ensure the proper performance of the BMS. Likewise, since the SoC estimation is usually performed at the cell-level, the SoC estimation algorithm must be computationally efficient to be feasible for estimation of SoC related to a large number of battery cells within a pack. The literature regarding battery SoC estimation is quite rich and can be broadly categorized into 1-traditional methods; 2-model-based methods; and 3-data-driven methods [4]. The traditional methods for SoC estimation are based on the Coulomb-Counting (CC) technique and open-circuit voltage (OCV) characteristics. The CC method is not accurate because the sensor errors can accumulate over time due to the current integration process [5]. In the OCV-based method, the relationship between the OCV and SoC is used to estimate the SoC. However, this technique cannot be applied in real-time vehicular applications because a relatively long rest time is needed before the OCV of the battery can be read [5]. The data-driven SoC estimation methods rely on extensive field testing to collect large battery datasets and apply algorithms that can learn from the data in order to represent the SoC in different operating regimes [4]. The disadvantage of the data-driven methods is related to the difficult, costly, and time-consuming training process that is needed to train the networks using a large amount of data [4]. The model-based methods utilize the battery model, e.g. electrochemical model or Equivalent Circuit Model (ECM) [6], together with a state estimator such as Kalman Filter and its derivations [7]-[8], Luenberger observer [9], sliding mode observer [10], particle filter [11], etc. Among different model-based methods, the techniques based on ECMs and filters achieve an acceptable performance level at a relatively low computational cost. Thus, these techniques are very popular in applications where real-time efficiency and cost factors are important. Some good review works have recently been published on the battery SoC estimation subject, which can be referred for more detailed review of the state-of-the-art [4],[12]. In short, the review of the state-of-the-art reveals that this subject has been widely studied in recent years, which shows that this topic is still an open problem and there are still some challenges that remain to be addressed. The Li-ion battery technology is very diverse with different cathode materials being used in its manufacture. Different Li-ion batteries thus represent different nonlinear behaviors with different complexity levels. Therefore, it is not possible to find a universal model and state estimator suitable for all types of batteries. The model and state estimator must be chosen and calibrated based on the target battery. In this paper, a general design procedure based on a system identification index, namely the Akaike information criterion

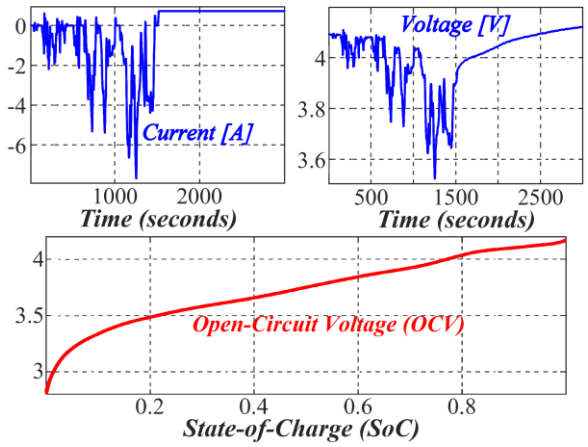

Fig. 1. Voltage-current validation data and open-circuit characteristics of the studied NMC-based Li-ion cells considering the WLTP cycle

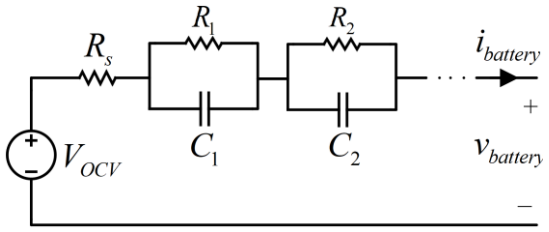

Fig. 2. The ECM of the battery

(AIC), is applied for modeling of the NMC-based Li-ion batteries. Additionally, based on the established battery Continuous Transfer Function (CTF), the EKF algorithm is used for estimation of the SoC of the studied cells. A series of Hardware-in-the-Loop (HiL) tests are also conducted to guarantee the embedded implementation feasibility. The modeling and SoC estimation methods are fully discussed in the following sections.

II. Experimental and System Identification Tests

A brief description of the experimental tests fulfilled to obtain the needed battery datasets as well as the procedure followed to model the target NMC-based Li-ion cells are presented in the following subsections.

A. Description of the Experimental Tests

The NMC-based Li-ion cells with rated voltage of 3.6 V and rated capacity of 3.4 Ah were used to obtain the required test datasets. The cells were discharged using the battery test system Digatron MCT and considering the World Harmonized Light-Duty Vehicle Test Procedure (WLTP) at different temperatures (15, 25, and 35). After WLTP discharge cycle, the cells were charged to 90% SoC with 0.68 A (0.2C), which was then followed by an idle period before iterating the tests. The cutoff voltage in charge and discharge processes were set to 4.2 V and 2.65 V, respectively. The terminal current and voltage waveforms of the battery recorded during the WLTP test cycle as well as the OCV-SoC curve at 25° C are shown in Fig. 1. More detailed information about the experimental tests can be found in [13].

B. System Identification Study for Battery Modeling

The structure of the battery ECM is shown in Fig. 2. It consists of a voltage source V_{OCV} representing the nonlinear relationship between the SoC and the open-circuit voltage, a series resistance R_S accounting for the instantaneous internal voltage drop of the battery, and a series of Resistive-Capacitive (RC) networks accounting for the charge transfer and ionic diffusion phenomena, where R_j and C_j denote the resistance and capacitance related to the *jth* RC network. In the general case, the linear part of the ECM can be represented with a transfer function model as follows:

$$G(s)=\frac{Y(s)}{U(s)}=\frac{b_0+b_1 s+b_2 s^2+\cdots+b_m s^m}{1+a_1 s+a_2 s^2+\cdots+a_n s^n} \quad (1)$$

where Y and U are the output and input s-polynomials (s being the Laplace notation) with degrees m and n, respectively. The battery current $i_{battery}$ and voltage $v_{battery}$ are considered as the system input U and system output Y, respectively. Likewise, the values of m and n represent the number of RC networks in the ECM. The model order is selected based on a system identification study using the AIC index. Because all models essentially contain an unavoidable uncertainty or error, one would expect that some part of the battery information will always be lost by the selected model. By estimating the relative quantity of the lost information in a given model, also known as model *Misfit*, the AIC helps to select a model with less information loss and thus, a model with higher quality:

$$AIC = 2N - 2\ln(\hat{L}) \quad (2)$$

where N is the number of parameters in the considered model and $\hat{L}$ is the maximum value of the likelihood function related to the given model. The model that leads to the least AIC value is generally preferred. The recorded battery dataset is used in the system identification analysis to select the appropriate model order. The results are shown in Fig. 3. As seen, the minimum AIC is obtained for the model with 20 parameters, i.e., m=9, n=10, which leads to an output variance of 0.000068. The results of Fig. 3 show that the model misfit can be significantly decreased by increasing N from 2 to 5. However, when N exceeds 5, the model misfit has only experienced a negligible improvement. Thus, to avoid undesirable computational overload, the model with 5 parameters, i.e., n=m=2 is chosen for the studied NMC-based Li-ion cells. To fit the battery data to the selected model, *MATLAB's System Identification* toolbox is used. The Levenberg-Marquardt algorithm is used for optimization. The

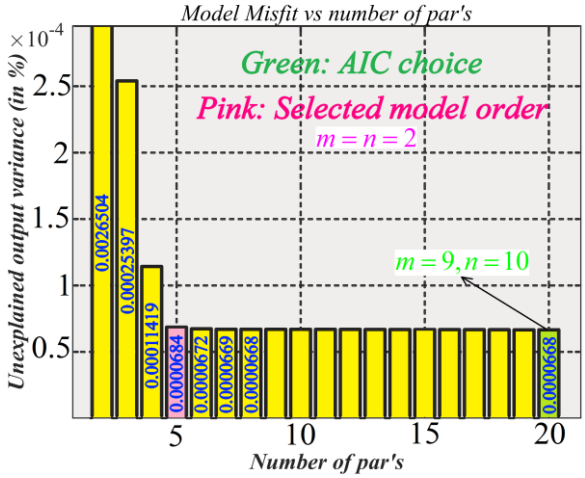

Fig. 3. Model order selection with AIC-based analysis

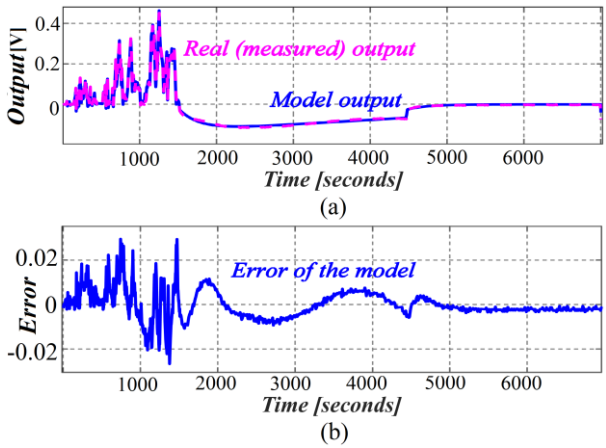

Fig. 4. Results of the system identification study. (a) Real (measured) and predicted (with the chosen model) outputs related to the impedance voltage drop. The impedance voltage drop is obtained by subtracting the terminal voltage from the internal cell voltage. (b) Relevant error signal

Mean Square Error (MSE) of the fitted model is obtained 3.691×10^{-5} and the model parameters are obtained as $a_1 = 1.983 \times 10^5$, $a_2 = 5.163 \times 10^7$, $b_0 = 5.937$, $b_1 = -1.646 \times 10^4$, and $b_2 = -2.868 \times 10^6$. The real and predicted values of the voltage across the impedance branch of the ECM are also shown in Fig. 4.

III. SoC Estimation with the EKF Algorithm

A. State-Space Representation of the Battery Model

The CTF model of the battery in (1) can be rewritten and divided into two different parts as follows:

$$G(s) = \frac{b_0 + b_1 s + b_2 s^2}{1 + a_1 s + a_2 s^2} = \frac{b_2}{a_2} + \underbrace{\frac{\alpha s + \beta}{1 + a_1 s + a_2 s^2}}_{Y'/U} \tag{3}$$

where α and β can be written as follows:

$$\alpha = \left(b_1 - \frac{a_1 b_2}{a_2}\right) \quad \beta = \left(b_0 - \frac{b_2}{a_2}\right)$$

In (3), multiplying Y'/U by the expression $\frac{Z}{Z}$ with Z being an auxiliary variable yields:

$$\frac{Y'(s)}{U(s)} = \frac{\alpha s + \beta}{1 + a_1 s + a_2 s^2} \times \frac{Z}{Z} \tag{4}$$

From (4), we can obtain the following equations:

$$\begin{aligned} Y'(s) &= (\alpha s + \beta) \times Z = \alpha \dot{Z} + \beta Z \\ U(s) &= \left(1 + a_1 s + a_2 s^2\right) \times Z = Z + a_1 \dot{Z} + a_2 \ddot{Z} \end{aligned} \tag{5}$$

where $\dot{Z}$ and $\ddot{Z}$ denote the first and second derivatives of Z, respectively. Defining $q_1 = Z$ and $q_2 = \dot{Z}$ as two state variables and using (5), two state equations an be obtained as follows:

$$\dot{q}_1 = q_2 \tag{6}$$

$$\dot{q}_2 = -\frac{a_1}{a_2} q_2 - \frac{1}{a_2} q_1 + \frac{U}{a_2} \tag{7}$$

Likewise, based on (5) and the defined state variables, y' can be rewritten as follows:

$$y' = \alpha q_2 + \beta q_1 \tag{8}$$

Also, the output equation of the CTF model can be obtained as follows:

$$y = \frac{b_2}{a_2} u + \alpha q_2 + \beta q_1 \tag{9}$$

Having obtained the state-space equations for the CTF part, the state-space equations for the whole battery system is obtained as:

$$\begin{aligned} \dot{q}_1 &= q_2 + \omega_1 \\ \dot{q}_2 &= -\frac{a_1}{a_2} q_2 - \frac{1}{a_2} q_1 + \frac{u}{a_2} + \omega_2 \\ \dot{q}_3 &= \frac{\eta \times u}{3600 \times Q} + \omega_3 \end{aligned} \tag{10}$$

where q_1, q_2, and q_3 are the state variables, ω_1, ω_2, and ω_3 are the process noises related to the first, second, and third state equations, respectively, η is the Coulombic efficiency (which is approximately considered 1 in this paper), Q is the capacity of the battery (in Ampere-hour), and u is the system input (current of the battery). In (10), the third state variable q_3 is equal to the SoC of the battery, i.e. $q_3 = SoC$. The output equation of the system $v_{battery}$ can also be written as follows:

$$\begin{aligned} v_{battery} = V_{OCV}(SoC) - \Bigg[&\frac{b_2}{a_2} u + \left(b_0 - \frac{b_2}{a_2}\right) q_1 \\ &+ \left(b_1 - \frac{a_1 b_2}{a_2}\right) q_2 \Bigg] + \nu \end{aligned} \tag{11}$$

where ν is the measurement noise. The noises are assumed to be Gaussian with covariance matrices H and R, respectively. The relationship between the V_{OCV} and SoC shown in Fig. 1 is approximated using the following polynomial function:

$$\begin{aligned} V_{OCV} = {} & 2025 SoC^9 - 9236 SoC^8 + \left(1.773 \times 10^4\right) SoC^7 \\ & - \left(1.865 \times 10^4\right) SoC^6 + \left(1.173 \times 10^4\right) SoC^5 - 4524 SoC^4 \\ & + 1063 SoC^3 - 148.3 SoC^2 + 12.75 SoC + 2.838 \end{aligned}$$

The above equation is obtained for battery stored at 25°C using MATLAB's curve fitting toolbox. A same procedure is used to obtain the open-circuit characteristics at 15°C and 35°C but the results are not shown here to shorten the paper.

B. Continuous EKF Algorithm

In the Continuous EKF (CEKF) algorithm, the measurement values between two sampling points will be inferred through interpolation. The state-space model of (10)-(11) can be written in the following form:

$$\begin{aligned} \dot{Q} &= f(Q, u, \omega, t) \\ y &= h(Q, \nu, t) \\ \omega &\sim (0, H) \\ \nu &\sim (0, R) \end{aligned} \tag{12}$$

where f and h are two nonlinear functions (which can be easily inferred from (10)-(11)) and u is the system input. Likewise,

$H^{3\times3}$ and R represent the covariance matrices of the process and measurement noises, respectively. The CEKF algorithm should be initialized at the first iteration, which is fulfilled as follows:

$$\hat{Q}_0^+ = E\left[Q(0)\right] = \begin{bmatrix} 0 & 0 & 0 \end{bmatrix}$$

$$\hat{P}_0^+ = E\left[\left(Q(0)-\hat{Q}(0)\right)\left(Q(0)-\hat{Q}(0)\right)^T\right] = \begin{bmatrix} 0.1 & 0 & 0 \\ 0 & 0.1 & 0 \\ 0 & 0 & 0.1 \end{bmatrix}$$

where Q is the state vector, $P^{3\times3}$ denotes the covariance matrix of the estimation error, and E is the expected value operator. Then, the partial derivative matrices at the current state estimate should be derived. Based on the state-space model of the battery, these matrices are obtained as:

$$F = \left.\frac{\partial f}{\partial q}\right|_{\hat{Q}} = \begin{bmatrix} 0 & 1 & 0 \\ -\frac{1}{a_2} & -\frac{a_1}{a_2} & 0 \\ 0 & 0 & 0 \end{bmatrix} \quad (13)$$

$$L = \left.\frac{\partial f}{\partial \omega}\right|_{\hat{Q}} = \begin{bmatrix} 1 & 0 & 0 \\ 0 & 1 & 0 \\ 0 & 0 & 1 \end{bmatrix} \quad (14)$$

$$C = \left.\frac{\partial h}{\partial q}\right|_{\hat{Q}} = \begin{bmatrix} \left(b_0 - \frac{b_2}{a_2}\right) & \left(b_1 - \frac{a_1 b_2}{a_2}\right) & \frac{\partial V_{OCV}}{\partial SoC} \end{bmatrix} \quad (15)$$

$$M = \left.\frac{\partial h}{\partial v}\right|_{\hat{Q}} = 1 \quad (16)$$

Then, the covariance matrices related to the process and measurement noises are updated using the following equations:

$$\tilde{H} = L \times H \times L^T \quad (17)$$

$$\tilde{R} = M \times R \times M^T \quad (18)$$

Finally, the time-update and measurement-update steps of the CEKF algorithm can be fulfilled through the following set of equations:

$$\dot{\hat{Q}} = f\left(\hat{Q}, u, \omega, t\right) + K\left(y - h\left(\hat{Q}, u, v, t\right)\right) \quad (19)$$

$$K = P \times C^T \times \tilde{R}^{-1} \quad (20)$$

$$P = FP + PF^T + \tilde{H} - PC^T \tilde{R}^{-1} CP \quad (21)$$

Since the CEKF algorithm is an iterative process, (13)-(21) keep repeating until the end of the simulation. The value of R is selected based on the accuracy level of the sensors, which typically can be found in the datasheet of the sensor [14]. Likewise, the value of H is chosen based on the trial and error, which is the approach followed by the majority of the existing works [15]-[18]. Accordingly, the values of R and H are set as:

$$R = 0.01 \quad H = diag\left(0.05, 0.05, 0.01\right) \quad (22)$$

IV. Experimental Results and Discussion

The developed algorithms are implemented in MATLAB/SIMULINK and the experimental test data are imported to the MATLAB workspace for testing of the proposed method. The sampling time of the algorithms is set to $T_s = 0.1s$. The obtained results are shown in Fig. 5. As seen in Fig. 5, the SoC is accurately tracked by the proposed SoC estimation mechanism and the terminal voltage of the battery is also accurately predicted by the EKF algorithm. At the beginning of the simulation, relatively large differences between the estimated and real values of the terminal voltage

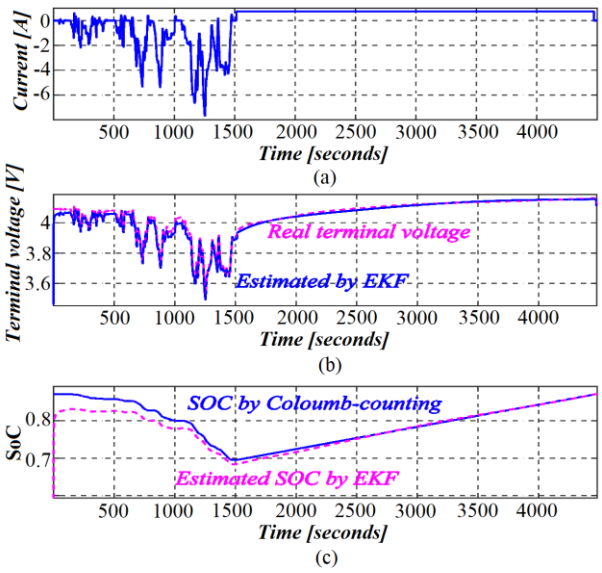

Fig. 5. (a) Current of the battery. (b) The measured and estimated values of the battery voltage. (c) The reference and EKF-based estimation of the SoC

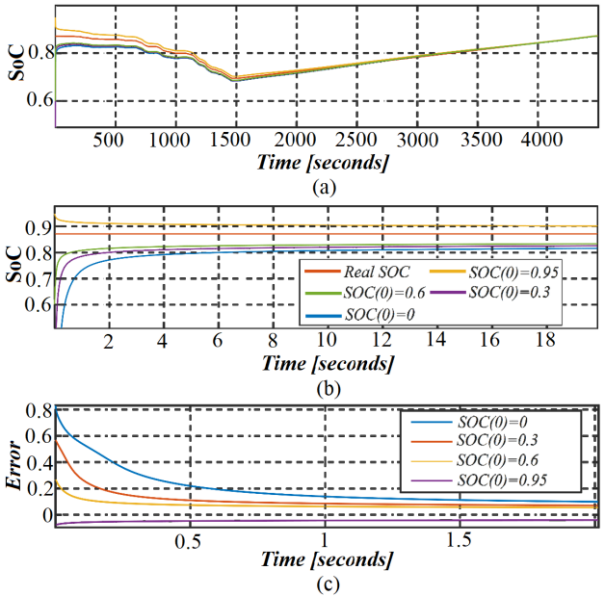

Fig. 6. (a) SoC estimation considering different initialization settings. (b) Expanded view of part (a). (c) SoC estimation error

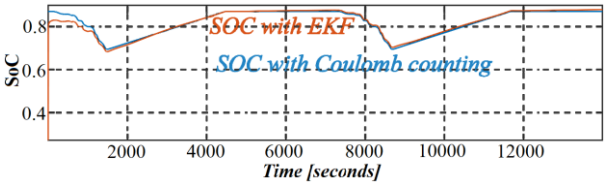

Fig. 7. SoC estimation over two iterations of the WLTP cycle

and SoC are observable, which are caused by setting the initial values of the state vector to zero. However, the filter properly converges to the true state value over the time and ultimately an appropriate state-estimation error below 2% can be achieved at the steady-state. To further evaluate the convergence of the filter, different initial SoC values are assigned in the CEKF algorithm. The obtained results are shown in Fig. 6. The CEKF is initialized with different values including $SoC(0)$=0, $SoC(0)$=0.3, $SoC(0)$=0.6, and $SoC(0)$=0.95. The results indicate that in all cases the estimated SoC accurately converges to the true SoC value. The SoC estimation results during two iterations of the WLTP cycle are also shown in Fig. 7, where it can again be confirmed that the filter has a stable and accurate performance. In the simulations, the convergence speed is a little bit slow because in Section III.B the initial value of the covariance matrix of the estimation error $\hat{P}_0^+$ is chosen to be very small. However, by increasing the value of the diagonal entries of the covariance matrix the convergence speed can be significantly enhanced. One should note that a very large initial value for $\hat{P}_0^+$ can also cause some unwanted overshoots in the estimation of states. Thus, the selection of the initial values should be fulfilled, carefully. To evaluate the computational burden of the proposed model and state estimation mechanism, some HiL tests using the dSPACE1104 development platform are also fulfilled. First, the C code of the developed algorithms are generated using MATLAB's Coder option. In the algorithms, the execution time is calculated using the dSPACE Real-Time Interface (RTI) through the so-called *atomic subsystems*. The relevant description file is then imported to the ControlDesk software for real-time evaluation of the codes. Considering the sampling time of $T_s = 0.1s$, the average execution time is calculated about 80 μs . Thus, no restriction regarding embedded implementation would exist in practice.

V. Conclusions

In this paper, modeling and SoC estimation of the NMC-based Li-ion battery cell is fulfilled. In the modeling phase, an efficient universal AIC-based system identification study is fulfilled and accordingly the CTF-based model of the battery is established. The state-space representation of the established model is then derived and used for SoC estimation of the cells using the CEKF algorithm, which yielded a SoC estimation error below 2%, while the average execution time of about $80\mu s$ is achieved when the sampling time is set to $T_s = 0.1s$. The proposed method can be applied for model order selection and SoC estimation of other battery types, as well. For future work, the authors will work toward developing an online parameter estimation method so the model parameters in the CEKF can be updated in real-time to account for the battery aging effects.

Acknowledgment

This work has been supported in part by Iran's National Elite's Foundation, in part by Electric Mobility Europe Call 2016 (ERA-NET COFUND) and Innovation Fund Denmark grant number 7064-00011B as part of the transnational eVolution2Grid (V2G) project.

References

[1] Y. Li, H. Sheng, Y. Cheng, D. I. Stroe, and R. H. Teodorescu, "State-of-health estimation of lithium-ion batteries based on semi-supervised transfer component analysis," *Applied Energy*, vol. 277, p. 115504, 2020.

[2] F. Naseri, E. Farjah, and T. Ghanbari, "An efficient regenerative braking system based on battery/supercapacitor for electric, hybrid, and plug-in hybrid electric vehicles with BLDC motor," *IEEE Transactions on Vehicular Technology*, vol. 66, no. 5, pp. 3724-3738, 2017.

[3] A. Gismero, D. I. Stroe, and E. Schaltz, "Calendar aging lifetime model for NMC-based lithium-ion batteries based on EIS measurements," *IEEE International Conference on Ecological Vehicles and Renewable Energies*, pp. 1-8, 2019.

[4] D. N. How, M. A. Hannan, M. H. Lipu, and P. J. Ker, "State of charge estimation for lithium-ion batteries using model-based and data-driven methods: A review," *IEEE Access*, vol. 7, pp. 136116-136136, 2020.

[5] S. Wang, C. Fernandez, C. Yu, Y. Fan, W. Cao, and D. I. Stroe, "A novel charged state prediction method of the lithium ion battery packs based on the composite equivalent modeling and improved splice Kalman filtering algorithm," *Journal of Power Sources*, vol. 471, p. 228450, 2020.

[6] F. Naseri, S. Karimi, E. Farjah, E. Schaltz, and T. Ghanbari, "Co-Estimation of supercapacitor states and parameters considering three-branch equivalent circuit model," *11th Power Electronics, Drive Systems, and Technologies Conference (PEDSTC)*, pp. 1-6, 2020.

[7] F. Naseri, E. Farjah, T. Ghanbari, Z. Kazemi, E. Schaltz, and J. L. Schanen, "Online parameter estimation for supercapacitor state-of-energy and state-of-health determination in vehicular applications," *IEEE Transactions on Industrial Electronics*, vol. 67, no. 9, pp. 7963-7972, 2020.

[8] R. Zhu, B. Duan, J. Zhang, Q. Zhang, and C. Zhang, "Co-estimation of model parameters and state-of-charge for lithium-ion batteries with recursive restricted total least squares and unscented Kalman filter," *Applied Energy*, vol. 277, p. 115494, 2020.

[9] S. Barsali, M. Ceraolo, J. Li, G. Lutzemberger, and C. Scarpelli, "Luenberger observer for lithium battery state-of-charge estimation," *ELECTRIMACS*, pp. 655-667, 2020.

[10] A. Nath, R. Gupta, R. Mehta, S. S. Bahga, A. Gupta, and S. Bhasin, "Attractive elipsoid sliding mode observer design for state of charge estimation of lithium-ion cells," *arXiv preprint* arXiv:2008.06871, 2020.

[11] Y. Wang and Z. Chen, "A framework for state-of-charge and remaining discharge time prediction using unscented particle filter," *Applied Energy*, vol. 260, p. 114324, 2020.

[12] G. L. Plett, "Review and some perspectives on different methods to estimate state of charge of lithium-ion batteries," *Journal of Automotive Safety and Energy*, vol. 10, no. 3, p. 249, 2019.

[13] A. Gismero, E. Schaltz, and D. I. Stroe, "Recursive state of charge and state of health estimation method for lithium-ion batteries based on coulomb counting and open circuit voltage," *Energies*, vol. 13, no. 7, p. 1811, 2020.

[14] Z. Kazemi, A. A. Safavi, F. Naseri, L. Urbas, and P. Setoodeh, "A secure hybrid dynamic state estimation approach for power systems under false data injection attacks," *IEEE Transactions on Industrial Informatics*, vol. 16, no. 12, pp. 7275-7286, 2020.

[15] Z. Kazemi, A. A. Safavi, S. Pouresmaeeli, and F. Naseri, "A practical framework for implementing multivariate monitoring techniques into distributed control system," *Control Engineering Practice*, vol. 82, pp. 118-129, 2019.

[16] S. Karimi, E. Farjah, T. Ghanbari, F. Naseri, and J. L. Schanen, "Estimation of parasitic capacitance of common mode noise in vehicular applications: an unscented Kalman filter-based approach," *IEEE Transactions on Industrial Electronics*, 2020.

[17] F. Naseri, E. Farjah, Z. Kazemi, E. Schaltz, T. Ghanbari and J. Schanen, "Dynamic Stabilization of DC Traction Systems Using a Supercapacitor-Based Active Stabilizer with Model Predictive Control," *IEEE Transactions on Transportation Electrification*, vol. 6, no. 1, pp. 228-240, 2020.

[18] T. Ghanbari, E. Farjah, F. Naseri, N. Tashakor, H. Givi, and R. Khayam, "Solid-State Capacitor Switching Transient Limiter based on Kalman Filter algorithm for mitigation of capacitor bank switching transients," *Renewable and Sustainable Energy Reviews*, vol. 90, pp. 1069-1081, 2018.